SUPPORTING INFORMATION

Mechanochemical Synthesis and Structural Analysis of Trivalent Lanthanide and Uranium Diphenylphosphinodiboranates

Taylor V. Fetrow and Scott R. Daly*

Department of Chemistry, The University of Iowa, E331 Chemistry Building, Iowa City, Iowa 52242, United States

Corresponding email: scott-daly@uiowa.edu

Table of Contents

Table S1. Single-crystal X-ray diffraction data for $U(H_3BPPh_2BH_3)_3$ (**1a**) and (**1b**), $Ce(H_3BPPh_2BH_3)_3$ (**2**), $Pr(H_3BPPh_2BH_3)_3$ (**3**), $Nd(H_3BPPh_2BH_3)_3$ (**4**), $Nd(H_3BPPh_2BH_3)_3(THF)_3$ (**4-THF**), $U(H_3BPH_2BH_3)I_2(THF)_3$ (**5**).

	1a	**1b**	**2**	**3**	**4**	**4-THF**	**5**
Formula	$C_{72}H_{96}B_{12}P_6U_2$	$C_{72}H_{96}B_{12}P_6U_2$	$C_{72}H_{96}B_{12}Ce_2P_6$	$C_{72}H_{96}B_{12}P_6Pr_2$	$C_{72}H_{96}B_{12}Nd_2P_6$	$C_{48}H_{72}B_6NdO_3P_3$	$C_{12}H_{24}B_2I_2O_3PU$
FW (g mol^{-1})	1753.08	1753.08	1557.26	1558.84	1565.5	999.06	760.73
crystal system	triclinic	monoclinic	triclinic	monoclinic	monoclinic	triclinic	orthorhombic
space group	P-1	$P2_1/c$	P-1	$P2_1/c$	$P2_1/c$	P-1	P*bcn*
a (Å)	11.4764(14)	18.8498(19)	11.4324(11)	37.239(4)	18.826(3)	11.5469(19)	9.5213(11)
b (Å)	12.8102(15)	9.6187(10)	12.7542(13)	9.6296(10)	9.6646(17)	14.970(3)	15.3494(17)
c (Å)	15.1334(18)	23.960(2)	28.438(3)	23.924(2)	23.904(4)	17.592(3)	15.8099(18)
α (deg)	104.030(5)	90	94.057(5)	90	90	97.233(5)	90
β (deg)	100.044(5)	109.622(5)	94.695(5)	107.636(5)	109.675(5)	96.868(5)	90
γ (deg)	107.371(5)	90	107.346(5)	90	90	111.125(5)	90
volume (Å)^3	1985.5(4)	4091.9(7)	3924.9(7)	8175.9(14)	4095.3(12)	2768.9(9)	2310.6(5)
Z	1	2	2	4	2	2	4
ρ_{calc} (g cm^{-3})	1.466	1.423	1.318	1.266	1.27	1.198	2.187
μ (mm^{-1})	4.232	4.107	1.306	1.332	1.408	1.059	9.77
F (000)	862	1724	1588	3184	1596	1038	1372
θ range (deg)	2.521/26.407	2.396/26.446	2.8725/27.865	1.703/26.431	2.293/26.313	2.061/26.352	2.517/28.278
R (int)	0.0488	0.0801	0.0508	0.1012	0.1449	0.0877	0.0427
data/restraints/parameters	8109/0/367	8365/625/399	18483/0/841	16695/42/712	8303/195/324	11206/24/493	2777/2/88
GOF	1.005	1.026	1.038	1.012	1.012	1.034	1.084
R_1 [$I > 2\sigma(I)$][a]	0.0384	0.0474	0.0381	0.0575	0.0679	0.0658	0.0548
wR_2 (all data)[b]	0.0787	0.1143	0.0704	0.124	0.1726	0.1634	0.1727
Largest Peak/Hole (e · Å^{-3})	1.916/-1.872	1.662/-1.989	2.151/-2.047	2.054/-1.241	0.775/-1.618	2.474/-1.268	4.078/-3.495
Temp (K)	150(2)	150(2)	100(2)	150(2)	150(2)	150(2)	150(2)

[a] $R_1 = \Sigma\, |F_o| - |F_c|\, | / |\Sigma|F_o|$ for reflections with $F_o^2 > 2\sigma(F_o^2)$.

[b] $wR_2 = [\Sigma w(F_o^2 - F_c^2)^2 / \Sigma(F_o^2)^2]^{1/2}$ for all reflections.

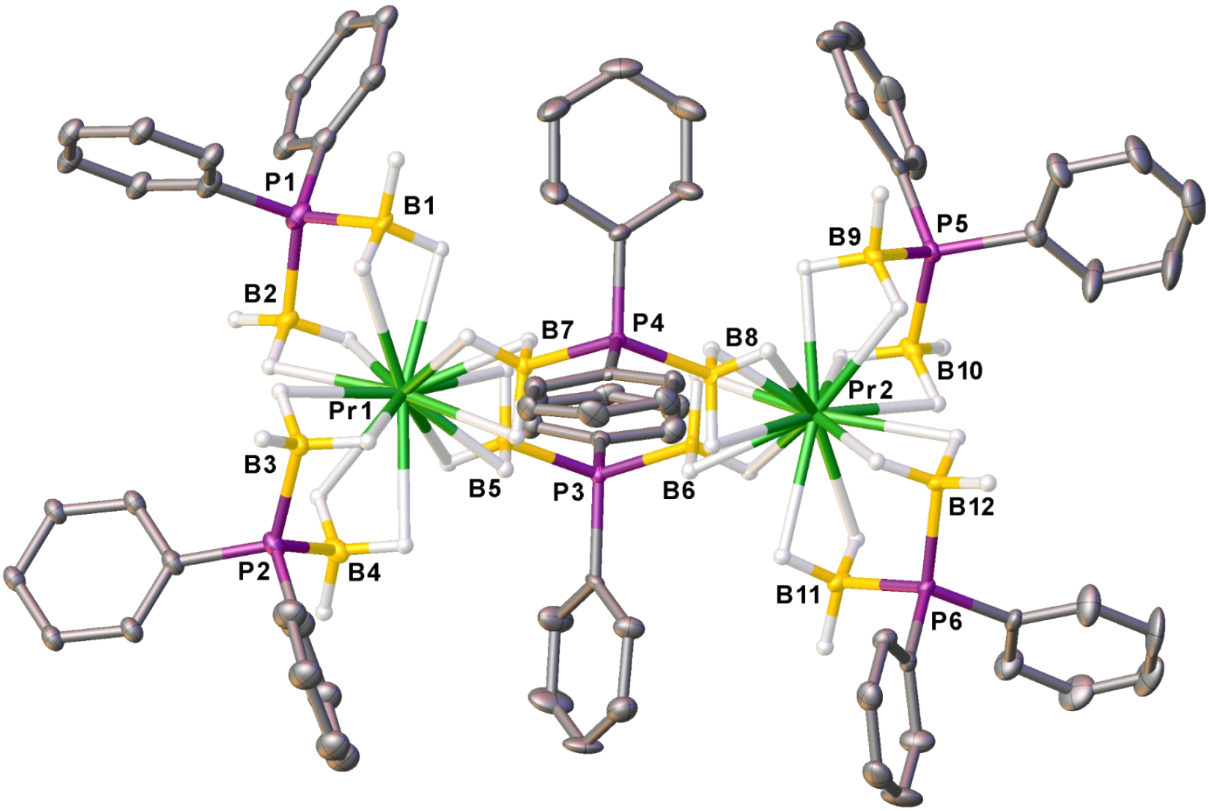

Figure S1. Molecular structure of $Pr(H_3BPPh_2BH_3)_3$ (**3**) with thermal ellipsoids shown at 35% probability. All phenyl hydrogen atoms were omitted from the figure.

NMR Spectra

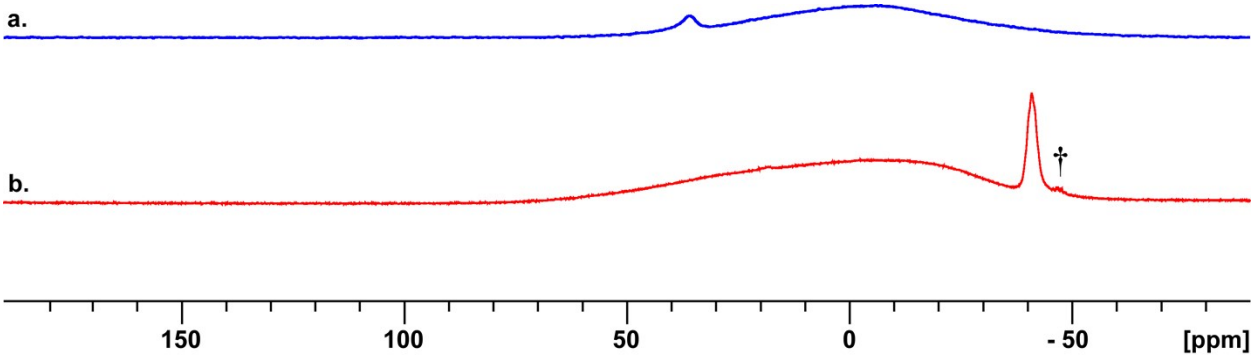

Figure S2. a) ^{11}B NMR spectra of crystalline $Nd(H_3BPPh_2BH_3)_3$ (**4**) in THF. b) ^{11}B NMR spectrum of NdI_3 and three equiv. of $K(H_3BPPh_2BH_3)$ stirred in 20 mL of THF for 24 h. The † is assigned to a small amount of hydrolysis.

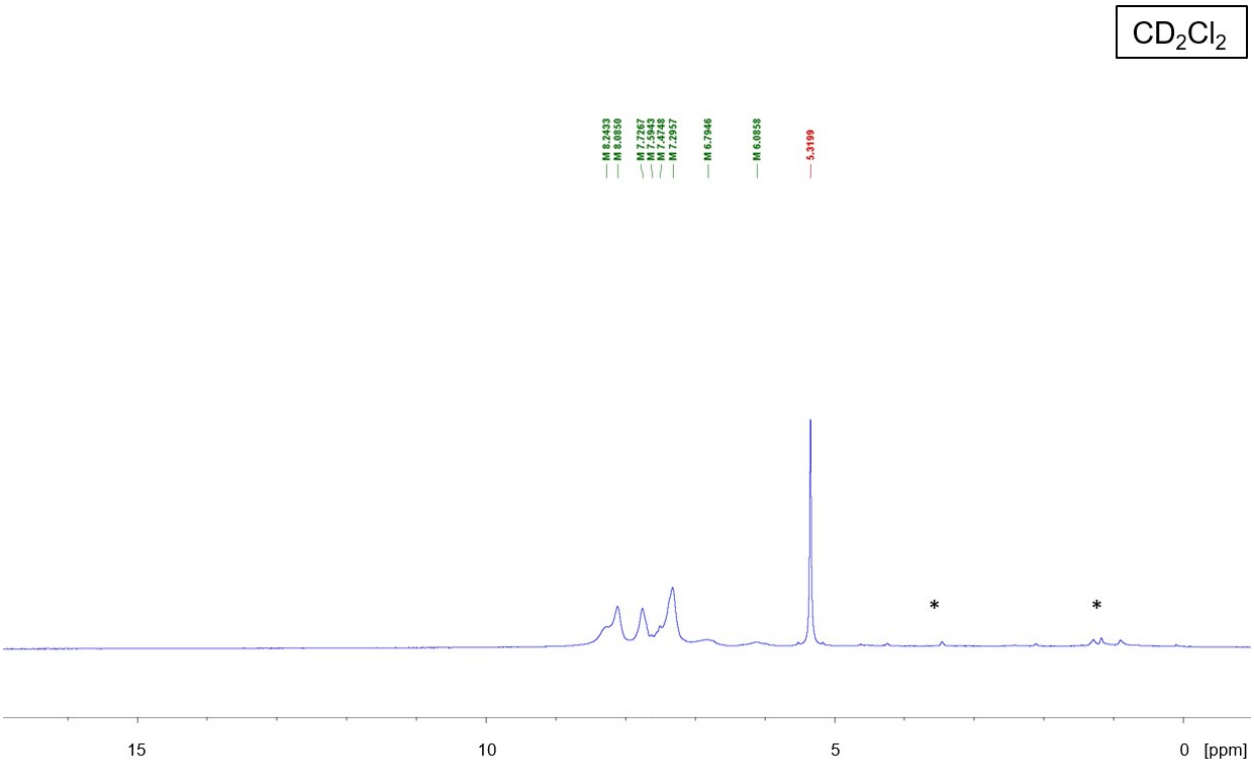

Figure S3. ^1H NMR spectrum of the phenyl resonances for $U(H_3BPPh_2BH_3)_3$ (**1a**) and (**1b**). The * symbol indicates resonances assigned to residual silicon grease, pentane, and Et_2O.

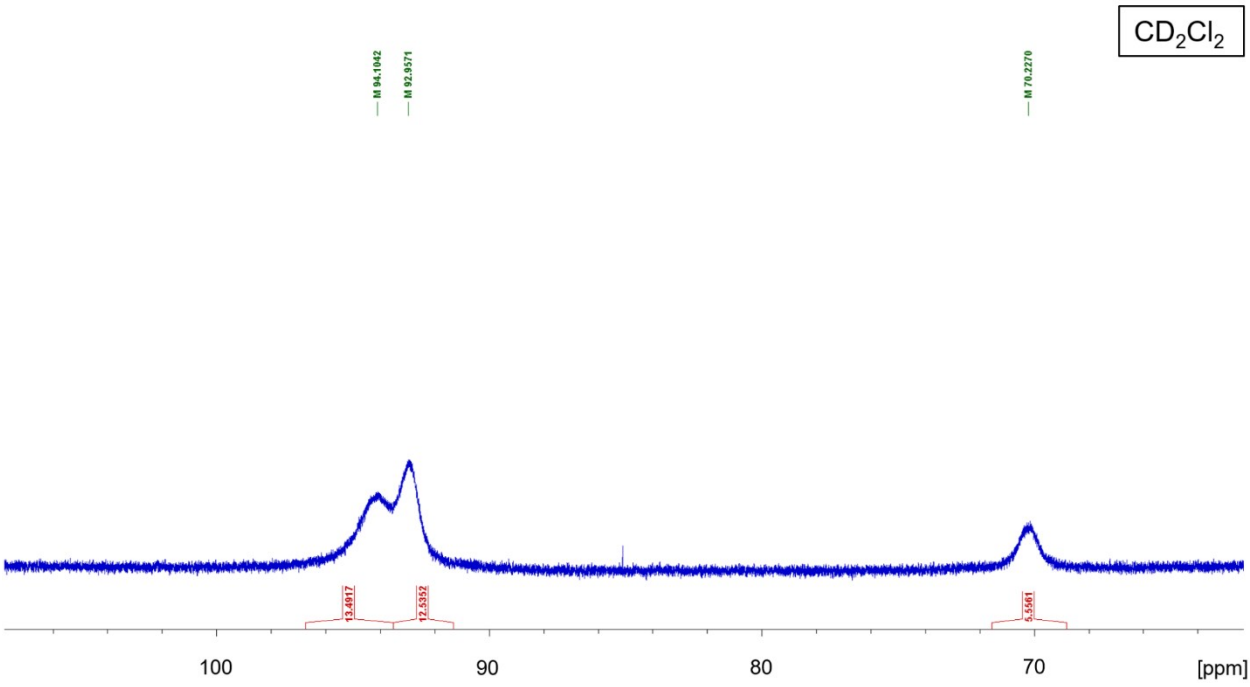

Figure S4. ^{1}H NMR spectrum of the BH_3 resonances for $U(H_3BPPh_2BH_3)_3$ (**1a**) and (**1b**).

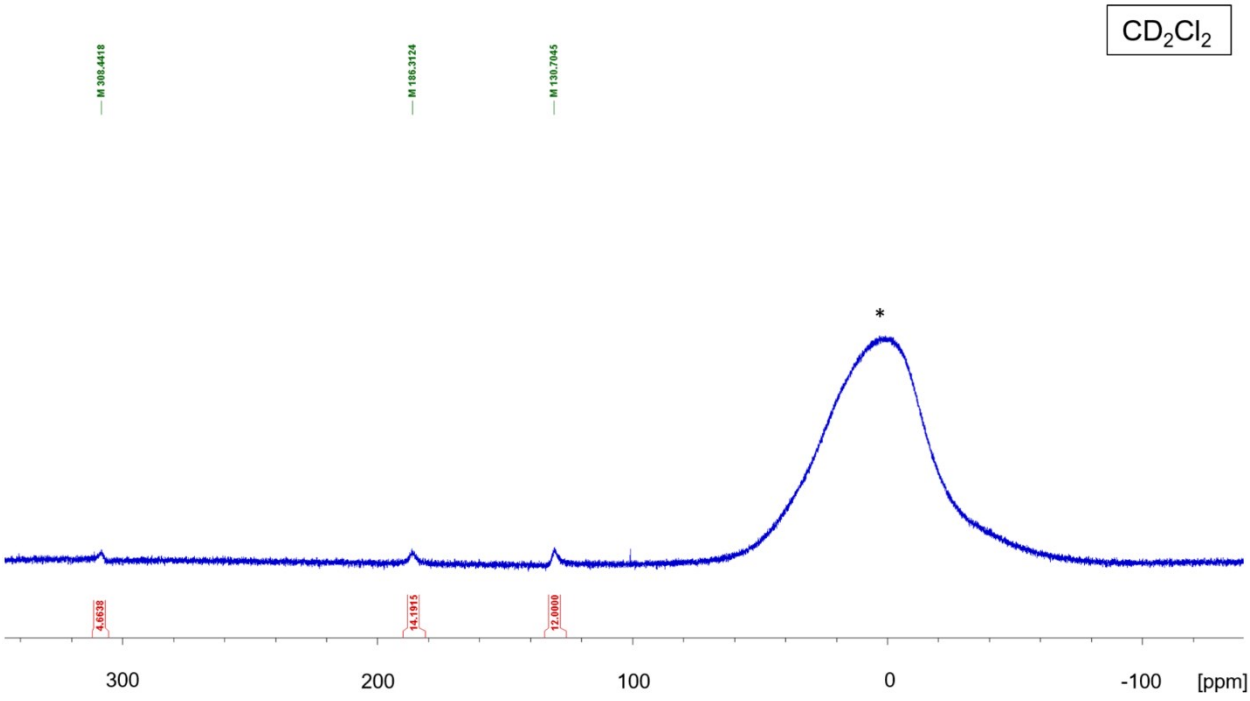

Figure S5. ^{11}B NMR spectrum of the BH_3 resonances for $U(H_3BPPh_2BH_3)_3$ (**1a**) and (**1b**). The * symbol indicates a resonance assigned to borosilicate within the instrument.

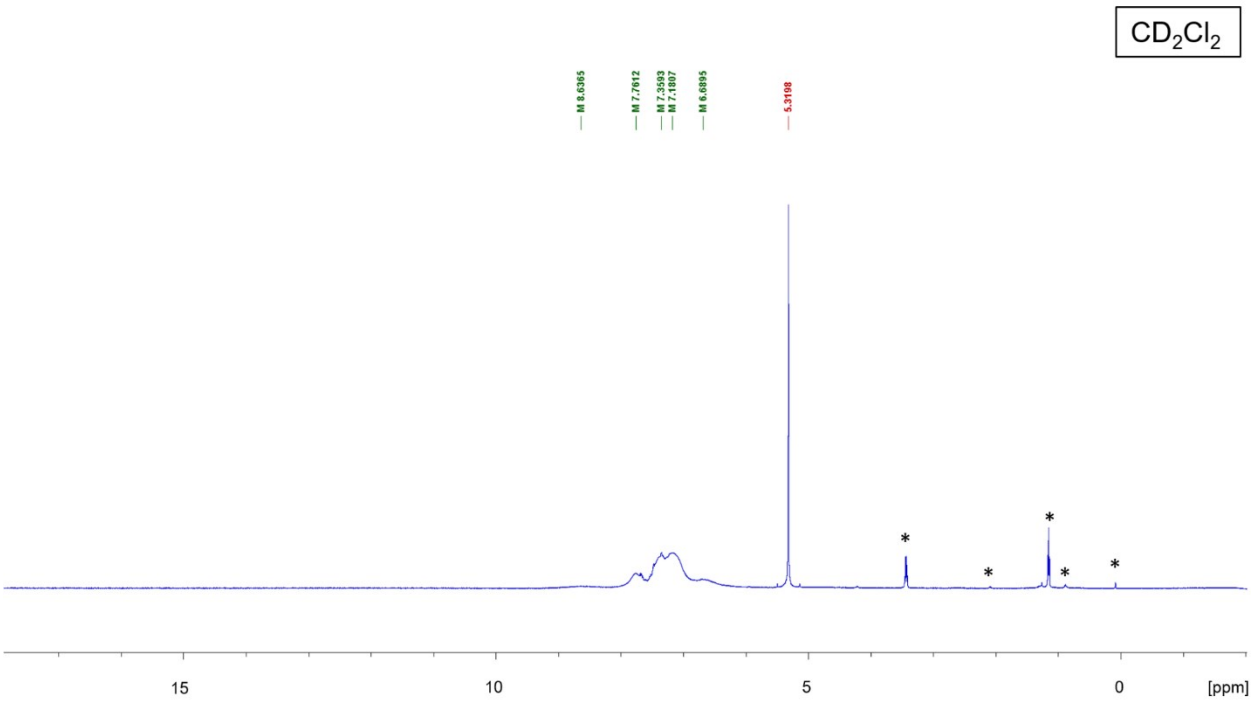

Figure S6. ^{1}H NMR spectrum of the phenyl resonances for $Ce(H_3BPPh_2BH_3)_3$ (**2**). The * symbol indicates resonances assigned to residual silicon grease, pentane, and Et_2O.

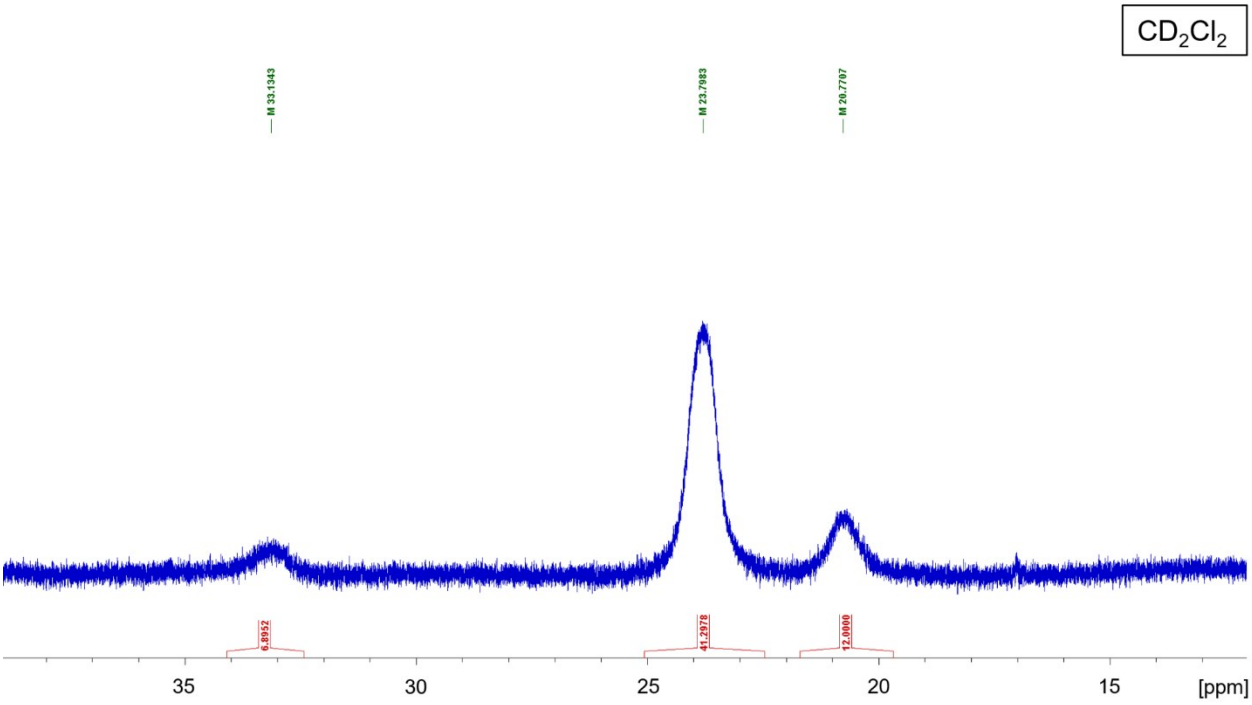

Figure S7. ^{1}H NMR spectrum of the BH_3 resonances for $Ce(H_3BPPh_2BH_3)_3$ (**2**).

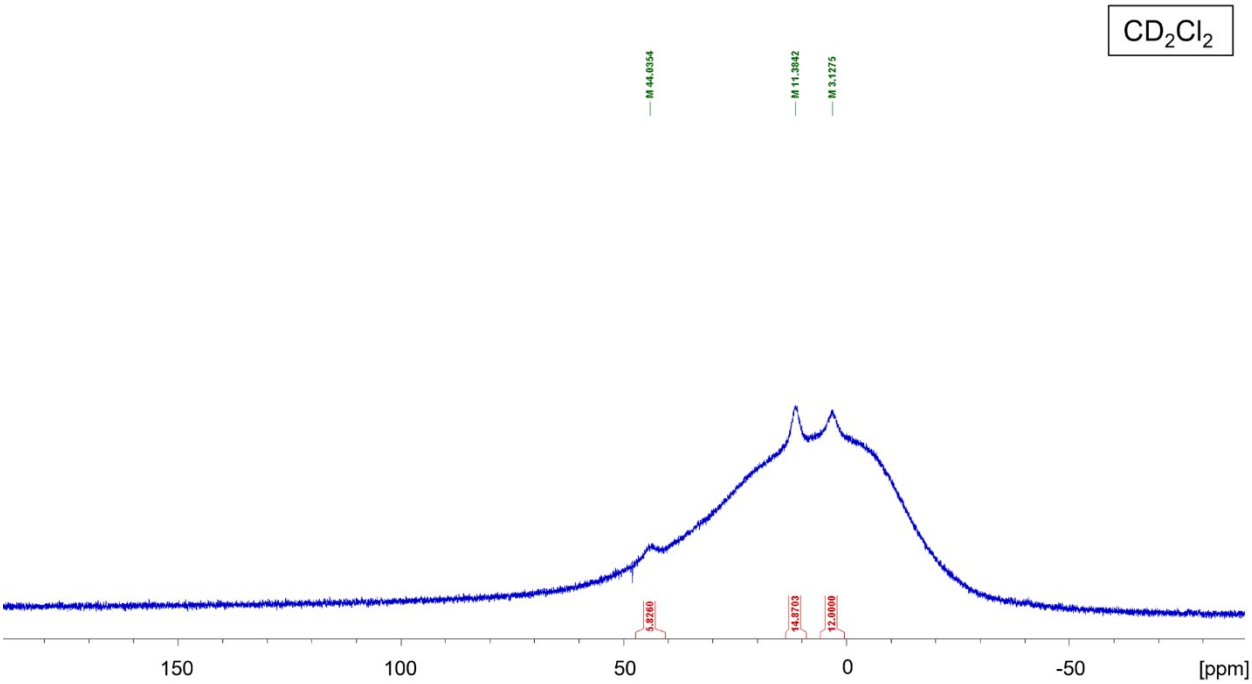

Figure S8. ^{11}B NMR spectrum of the BH_3 resonances for $Ce(H_3BPPh_2BH_3)_3$ (**2**). The large broad feature extending from δ 80 to -50 is assigned to borosilicate inside of the instrument.

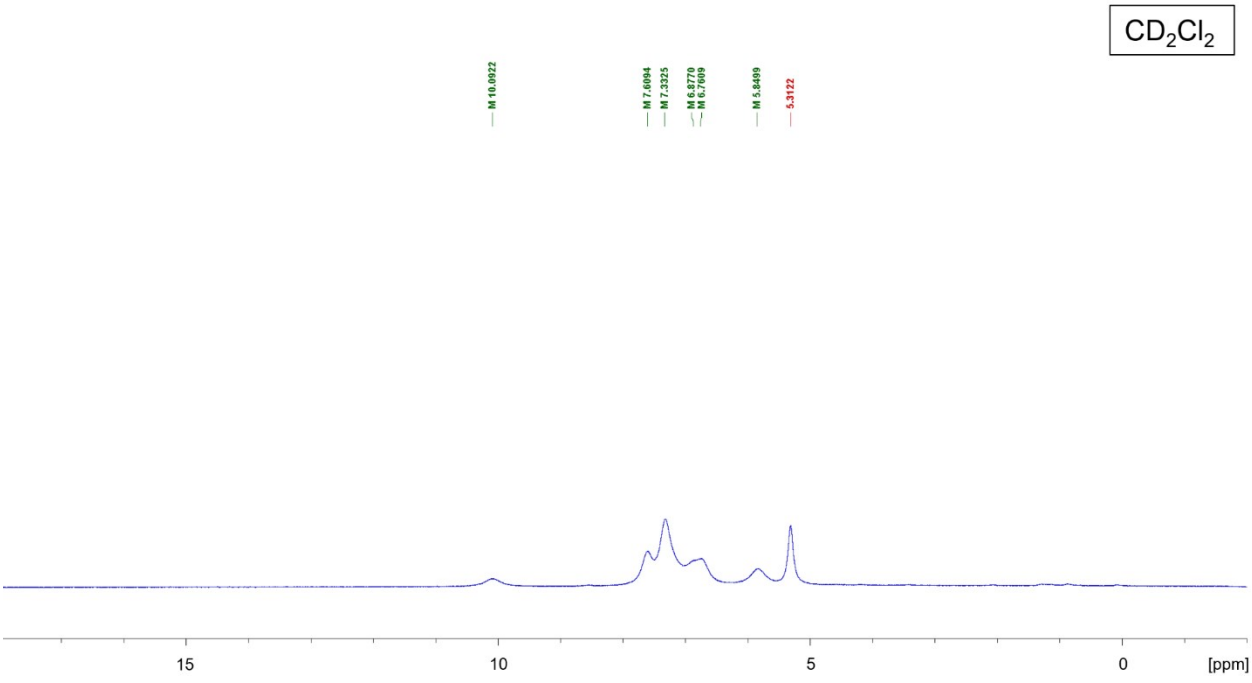

Figure S9. ^{1}H NMR spectrum of the phenyl resonances for $Pr(H_3BPPh_2BH_3)_3$ (**3**).

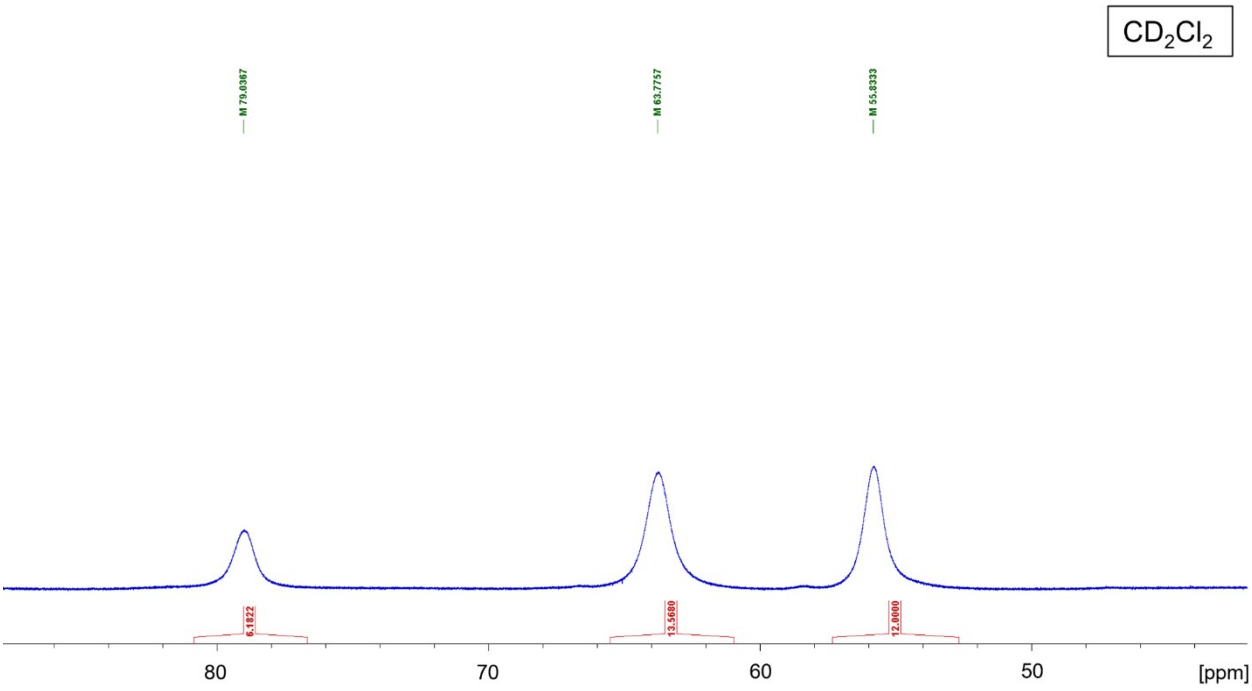

Figure S10. ^{1}H NMR spectrum of the BH_3 resonances for $Pr(H_3BPPh_2BH_3)_3$ (**3**).

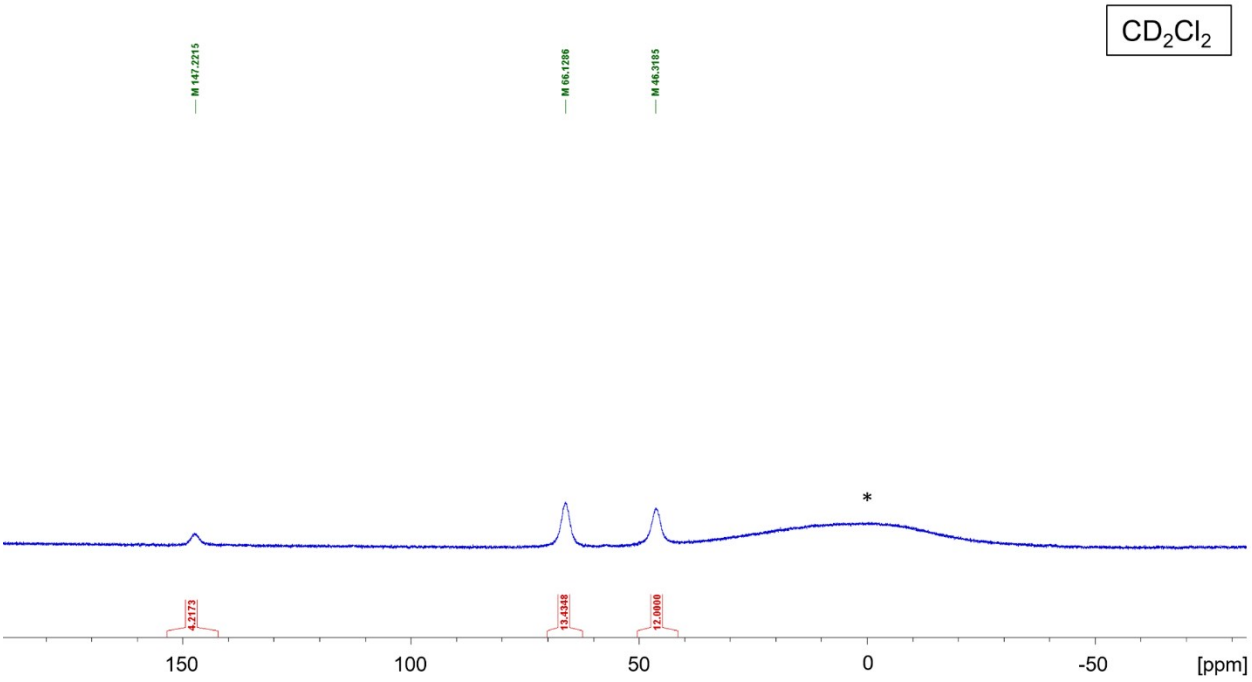

Figure S11. ^{11}B NMR spectrum of the BH_3 resonances for $Pr(H_3BPPh_2BH_3)_3$ (**3**). The * symbol indicates a resonance assigned to borosilicate within the instrument.

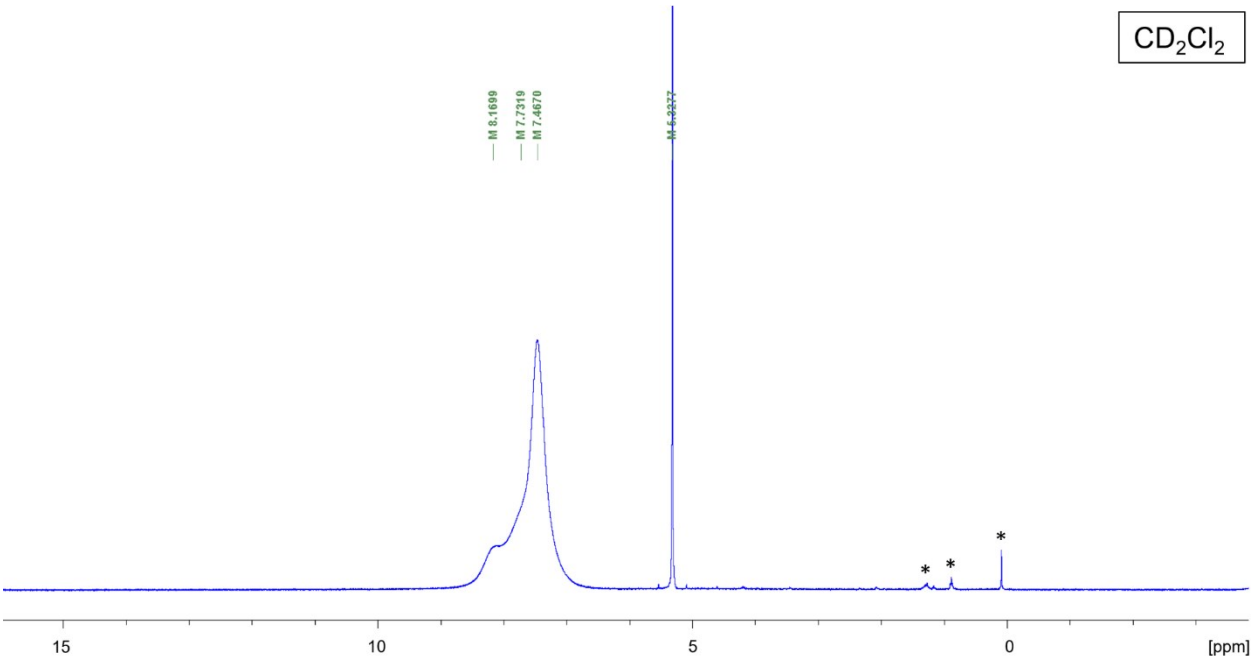

Figure S12. ^{1}H NMR spectrum of the phenyl resonances for $Nd(H_3BPPh_2BH_3)_3$ (**4**). The * symbol indicates resonances assigned to residual silicon grease and pentane.

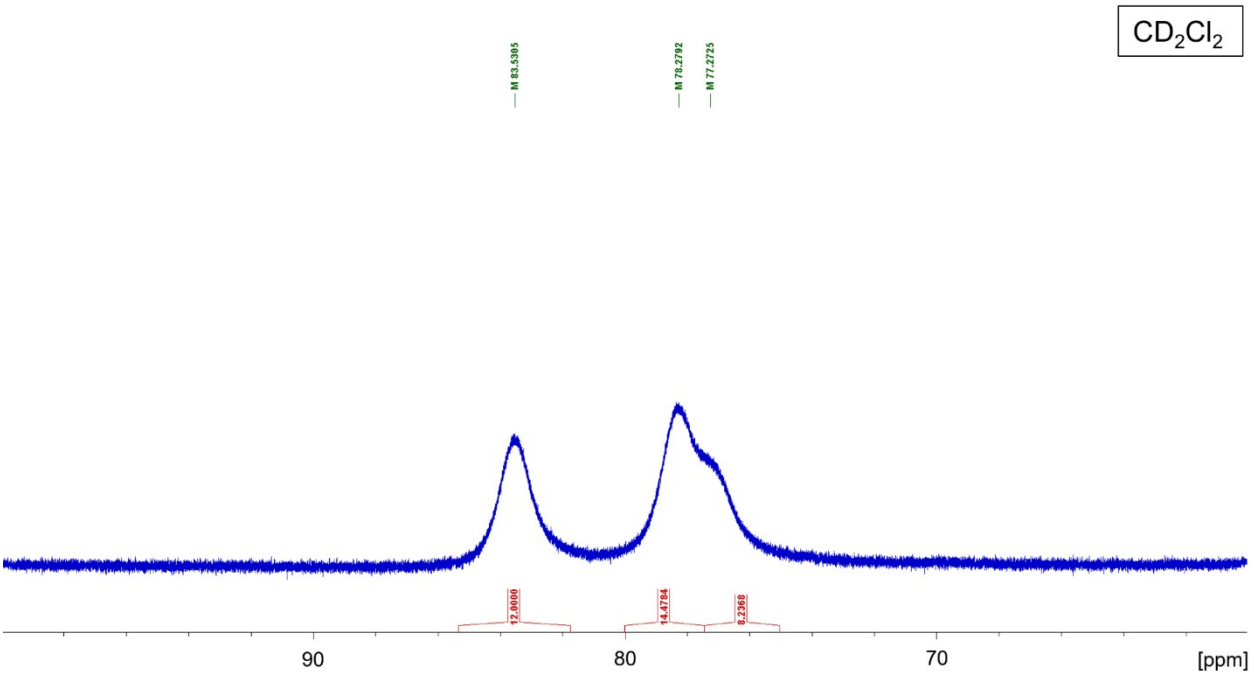

Figure S13. ^{1}H NMR spectrum of the BH_3 resonances for $Nd(H_3BPPh_2BH_3)_3$ (**4**).

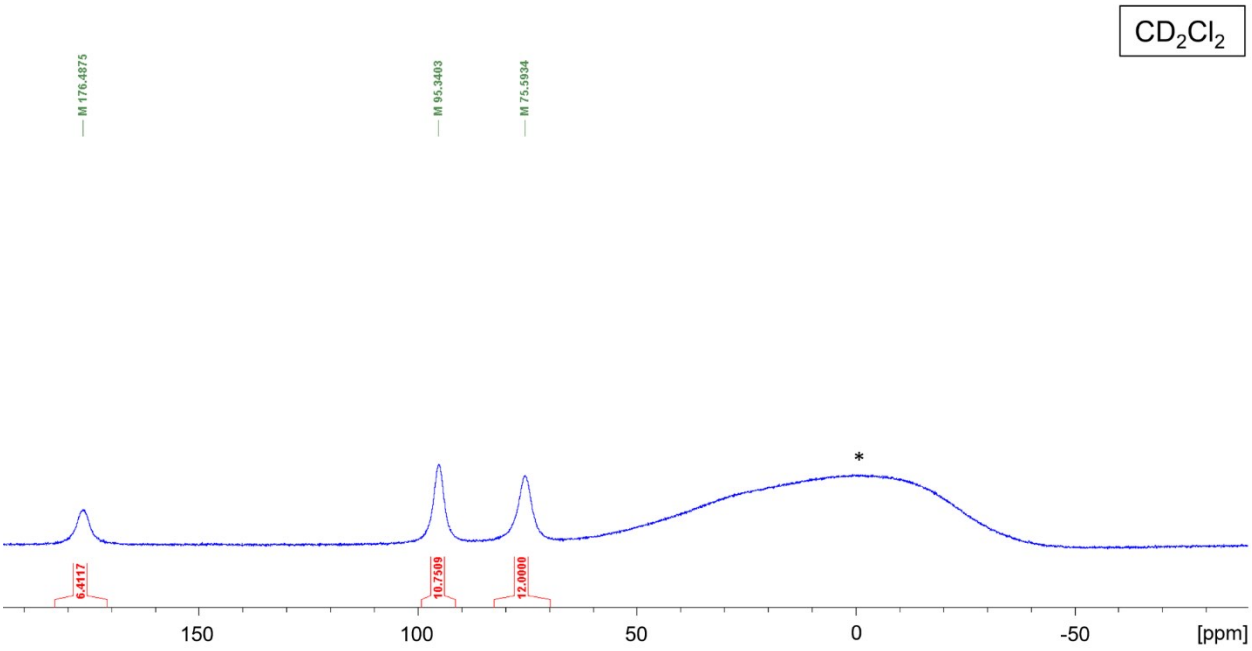

Figure S14. ^{11}B NMR spectrum of the BH_3 resonances for $Nd(H_3BPPh_2BH_3)_3$ (**4**). The * symbol indicates a resonance assigned to borosilicate within the instrument.

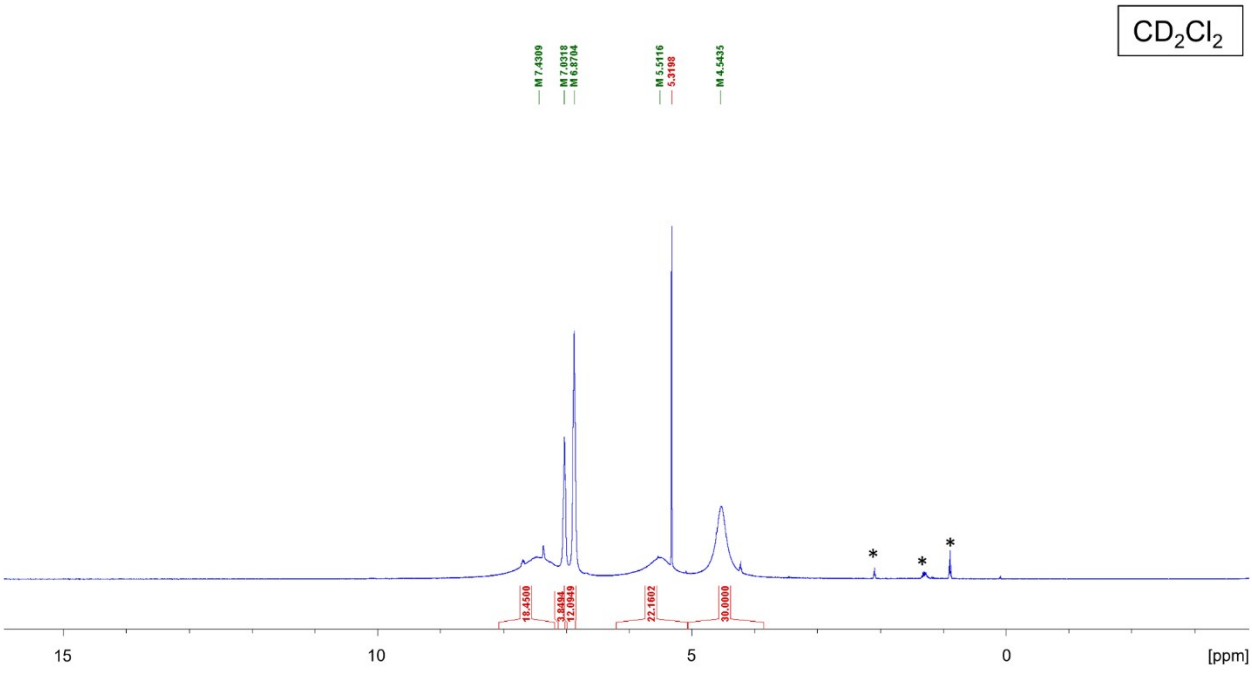

Figure S15. ^{1}H NMR spectrum of the phenyl and THF resonances for $Nd(H_3BPPh_2BH_3)_3(THF)_3$ (**4-THF**). The * symbol indicates resonances assigned to residual Et_2O and pentane.

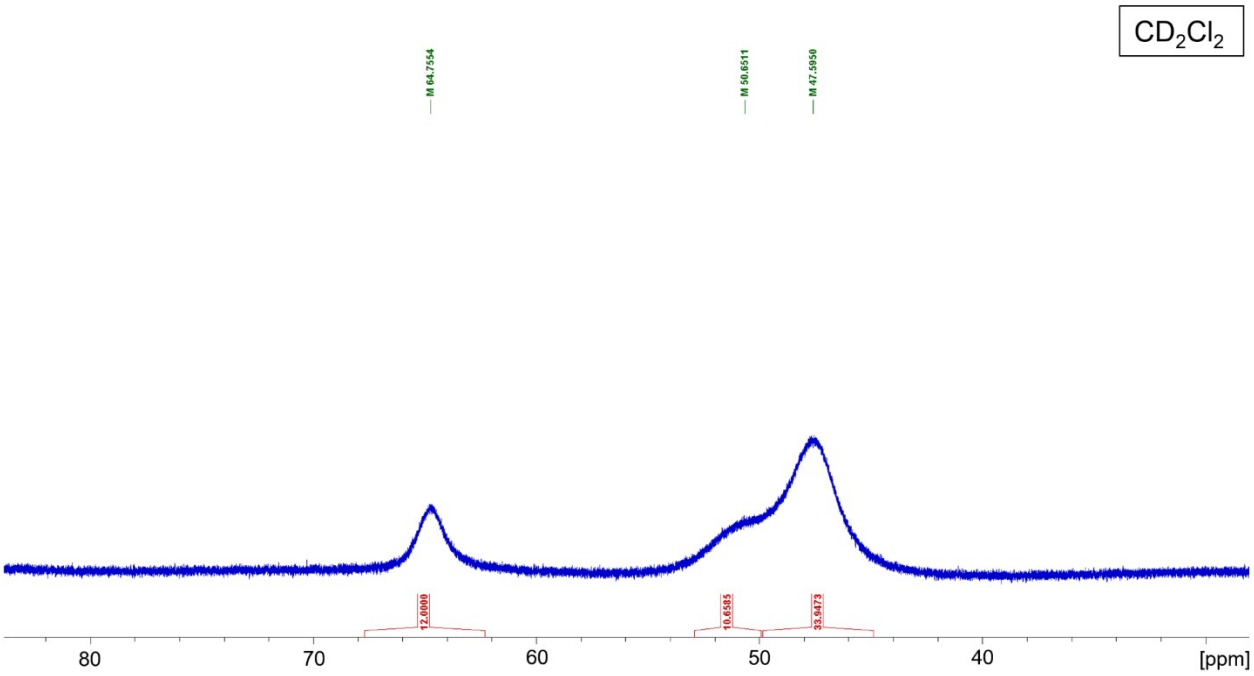

Figure S16. ^{1}H NMR spectrum of the BH_3 resonances for $Nd(H_3BPPh_2BH_3)_3(THF)_3$ (**4-THF**).

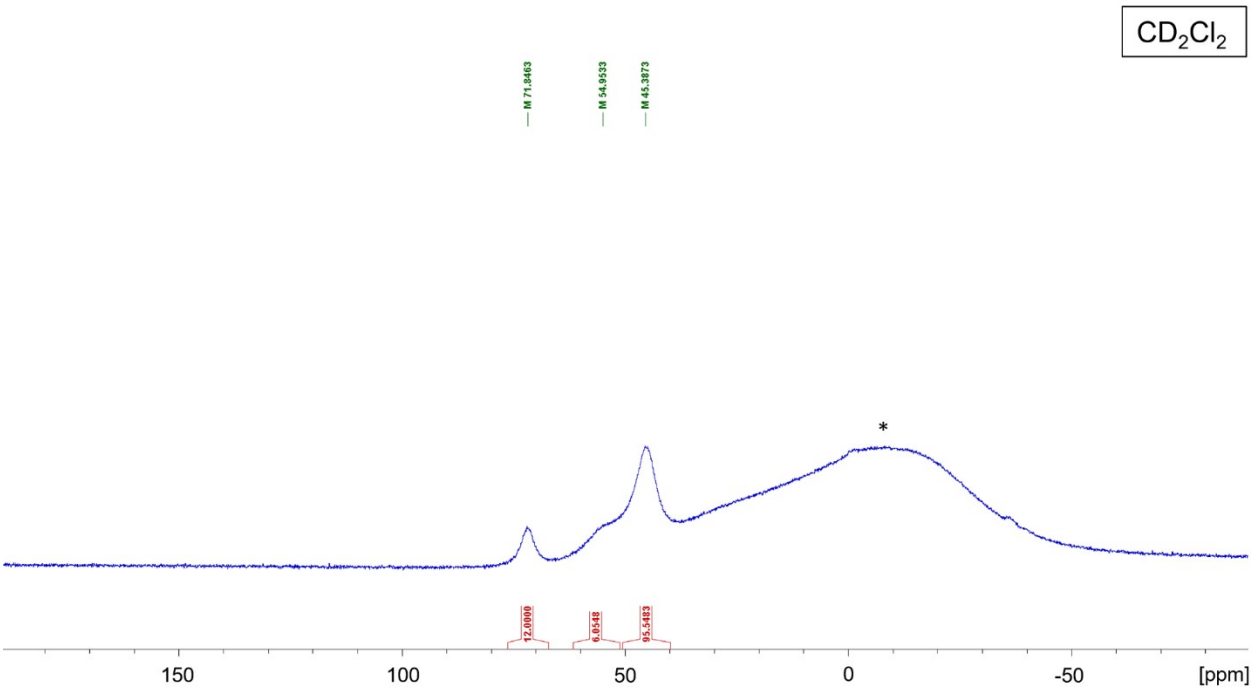

Figure S17. ^{11}B NMR spectrum of the BH_3 resonances for $Nd(H_3BPPh_2BH_3)_3(THF)_3$ (**4-THF**). The * symbol indicates a resonance assigned to borosilicate within the instrument.

IR (ATR) Spectra

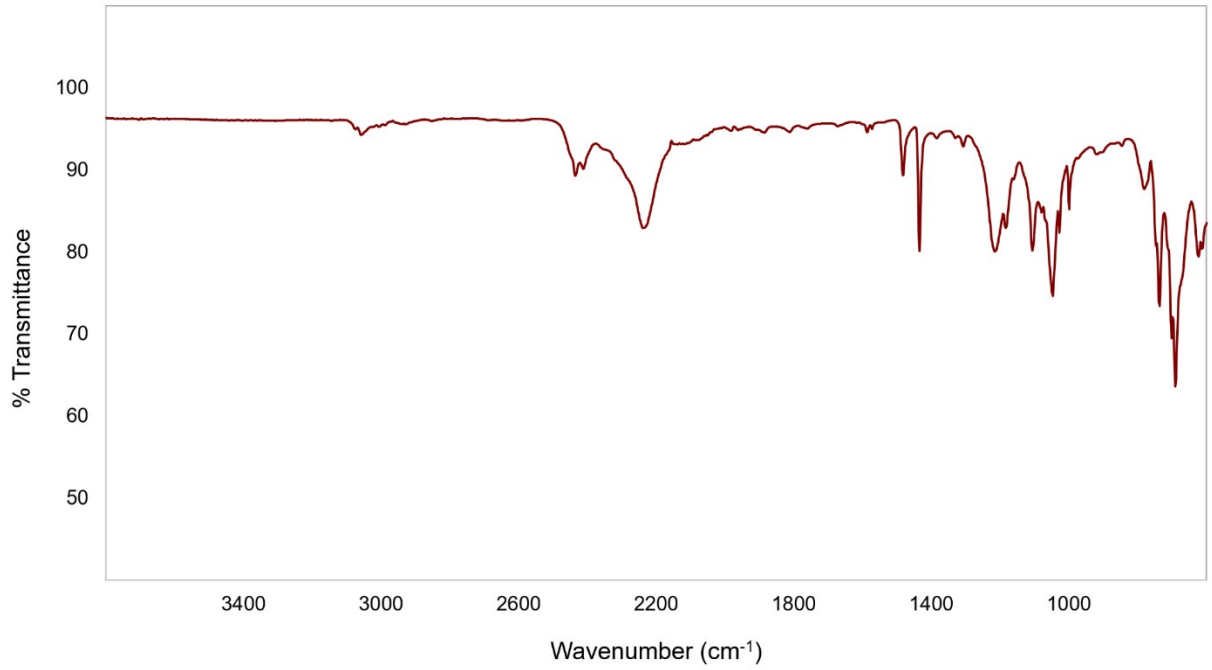

Figure S18. FTIR spectrum (ATR) for $U(H_3BPPh_2BH_3)_3$ for **1a** and **1b**.

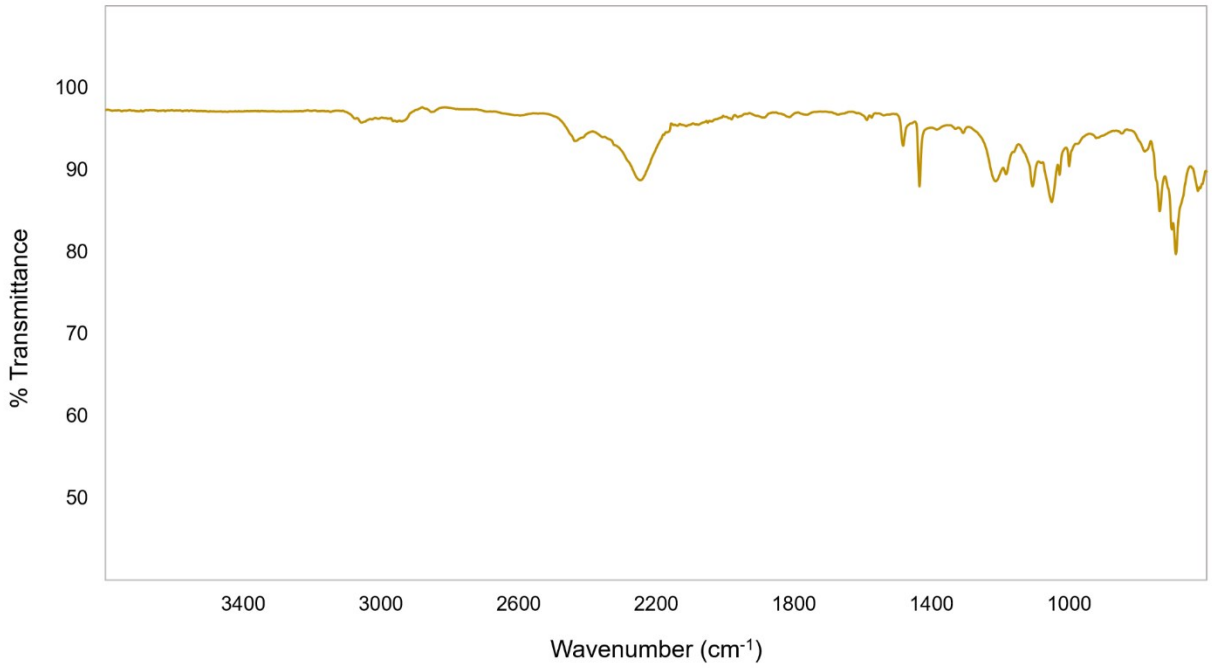

Figure S19. FTIR spectrum (ATR) for $Ce(H_3BPPh_2BH_3)_3$ (**2**).

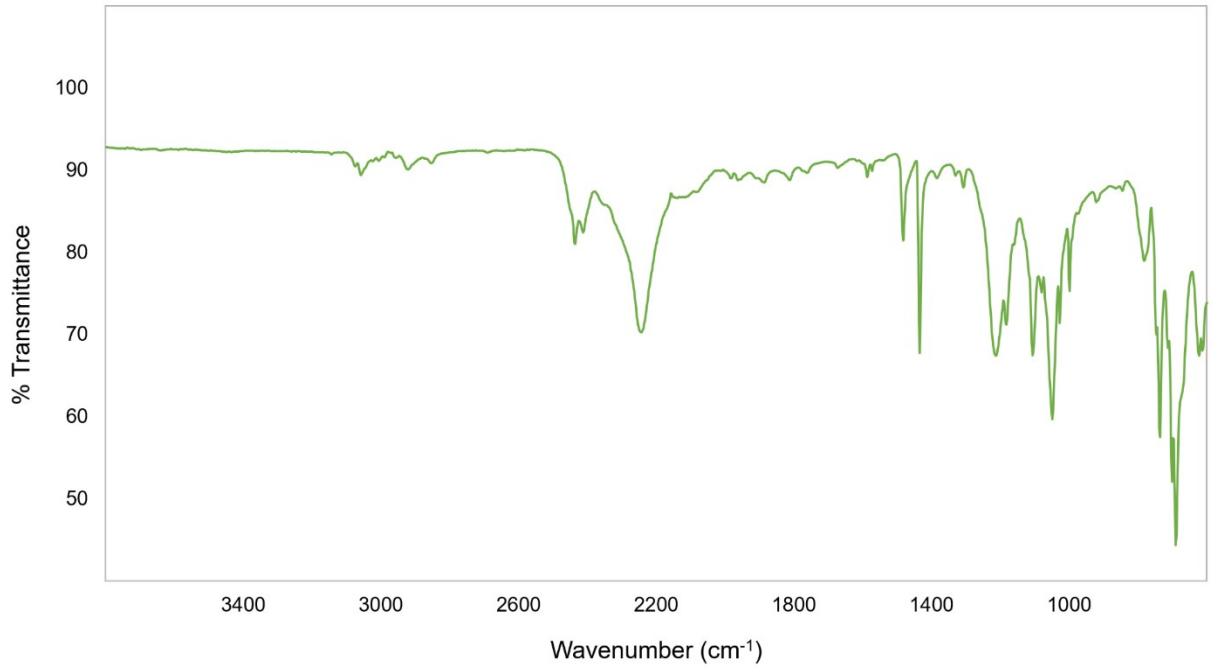

Figure S20. FTIR spectrum (ATR) for $Pr(H_3BPPh_2BH_3)_3$ (**3**).

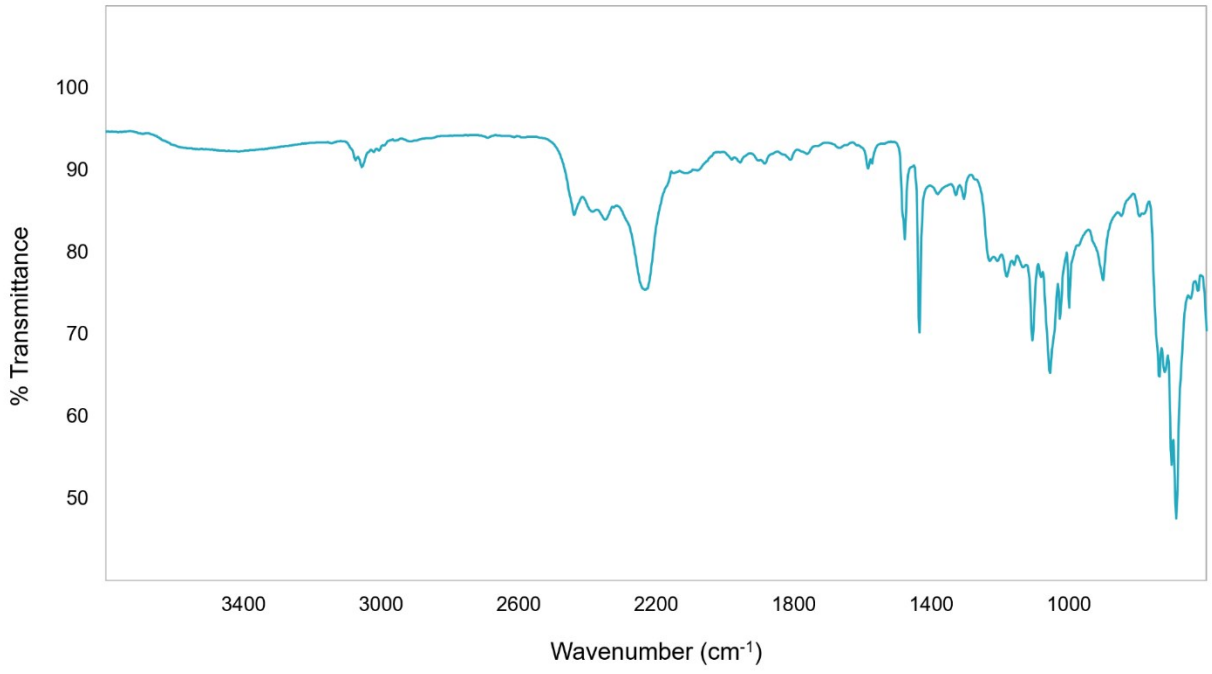

Figure S21. FTIR spectrum (ATR) for $Nd(H_3BPPh_2BH_3)_3$ (**4**).

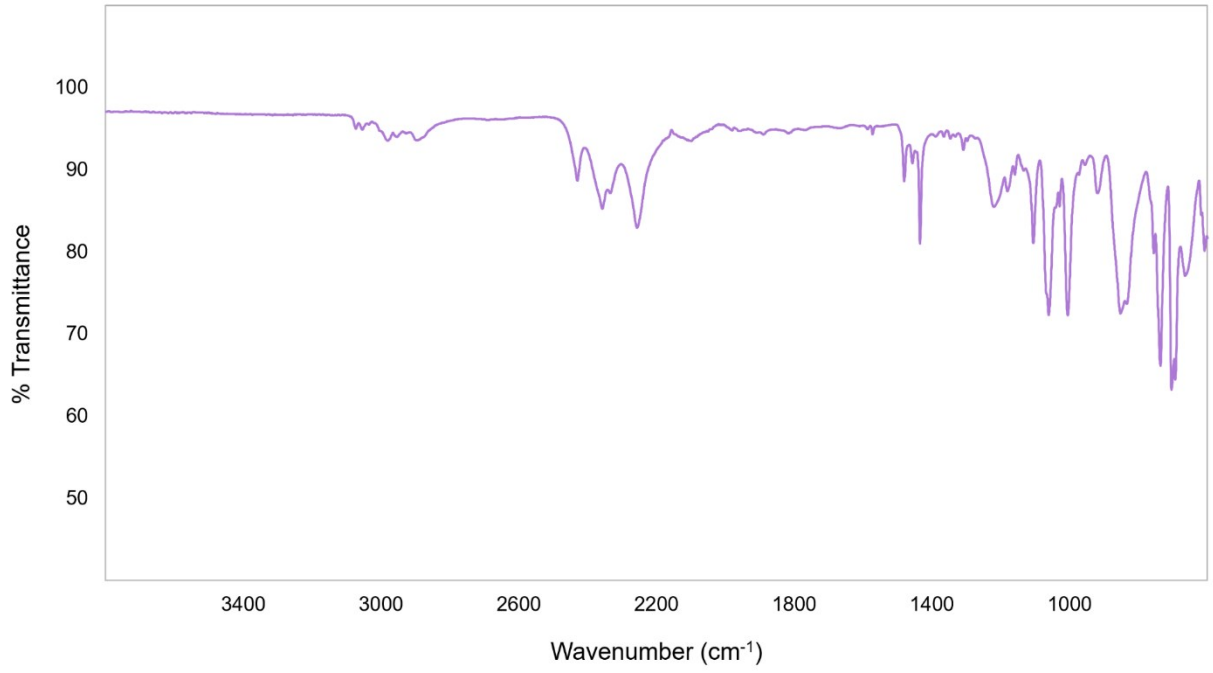

Figure S22. FTIR spectrum (ATR) for $Nd(H_3BPPh_2BH_3)_3(THF)_3$ (**4-THF**).

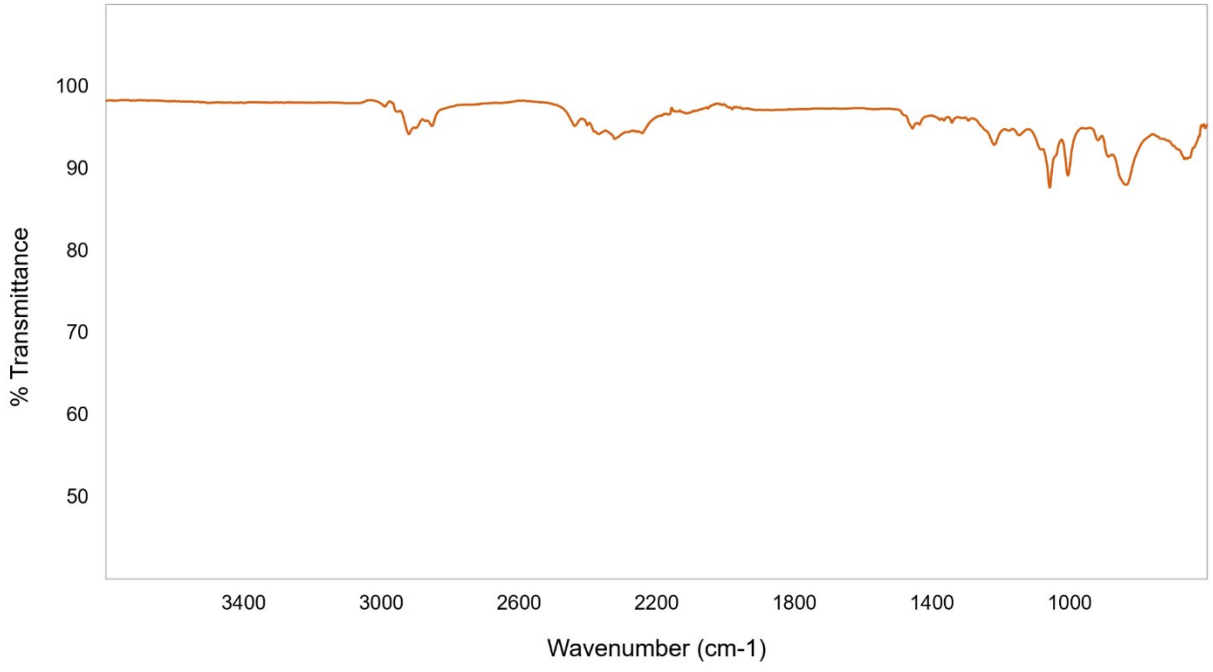

Figure S23. FTIR spectrum (ATR) for $U(H_3BPH_2BH_3)_3I_2(THF)_3$ (**5**).